

# Strains in Sand Due to Cyclic Loading in Triaxial Conditions

**Andrzej Sawicki, Jacek Mierczyński, Waldemar Świdziński**

Institute of Hydro-Engineering PAS, ul. Kościarska 7, 80-328 Gdańsk-Oliwa, Poland,  
e-mail: as@ibwpan.gda.pl

(Received June 09, 2009; revised July 20, 2009)

## Abstract

The experimental results dealing with the cyclic loading of sand samples in triaxial conditions are presented. These results show the development of both the volumetric and deviatoric permanent strains due to a large number of loading cycles. The analysis of experimental data has led to the formulation of semi-empirical constitutive equations, expressed in the incremental form, for these strains as functions of the cyclic shear stress amplitude, number of loading cycles and the initial stress state, around which the cyclic shearing takes place.

**Key words:** cyclic loadings, granular soils, permanent strains, triaxial conditions.

## 1. Introduction

The present paper deals with investigations on strains that develop in sands due to cyclic loadings. This problem, particularly the cyclic loading compaction, has been investigated in geotechnical engineering for many years, because of its practical importance. Review of respective literature is presented in the state-of-the-art paper by Sawicki and Mierczyński (2006) or in the book by Ishihara (1996). Long time ago, the senior author of this paper proposed a simple model of compaction/liquefaction of granular soils caused by cyclic loads, Sawicki (1987). Then, that model has been successfully applied to analyse various problems of engineering importance, e.g. Sawicki and Świdziński (2007), see also references in Sawicki and Mierczyński (2006).

The simplicity of the the compaction/liquefaction model was achieved due to its non-complicated structure, and a straightforward method of calibration. The key role in the model of compaction/liquefaction is played by the so-called common compaction curve. This curve is determined from the simple cyclic shearing tests, performed at different cyclic shear strain amplitudes. As a result of such tests, one obtains the compaction curves, i.e. the curves representing the permanent volumetric strains as functions of the number of loading cycles  $N$ . For each value of the cyclic shear strain amplitude  $\gamma_0$  one obtains a different curve  $\Phi = \Phi(N)$ , where

$\Phi = \varepsilon_v^p(1 - n_0)/n_0 =$  compaction,  $n_0 =$  initial porosity and  $\varepsilon_v^p =$  permanent volumetric strain. In this paper the soil mechanics convention is applied, where the plus sign denotes compression. If such distinct compaction curves are plotted on the  $(z, \Phi)$  plane, where  $z = \gamma_0^2 N/4$ , one obtains a single common curve as shown in Fig. 1. The data shown in this Figure correspond to simple cyclic shearing tests. Similar common compaction curves were obtained for the data presented by other authors, e.g. Martin et al (1975), Nemat-Nasser and Shokooh (1979), Sawicki and Mierczyński (2006).

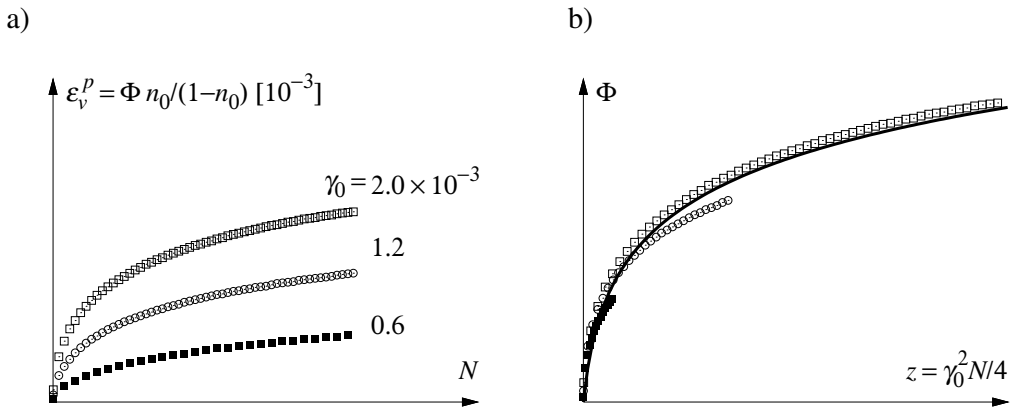


**Fig. 1.** Densification curves obtained in a simple cyclic shearing at different cyclic shear strain amplitudes (a); Common compaction curve for the data from Fig. 1a (b)

Further investigations have shown that the common compaction curve approximates well the densification of sand just up to tens of loading cycles, see Niemunis (2003), Świdziński and Mierczyński (2006). For a number of loading cycles  $N \geq 10^2$  the experimental data do not fit to a single curve as that shown in Fig. 1b. Therefore, a more general approach to the problem of permanent strains that develop during the cyclic loading of granular soils is necessary.

Such an approach should take into account more features influencing densification than a simple model of compaction/liquefaction, already mentioned. Careful analysis of experimental data shows that the initial static stress state, around which the cyclic loading occurs, is an important factor that influences the development of permanent strains due to cyclic loading. Our experimental investigations have shown that during the cyclic loading, not only the permanent volumetric strains develop, but there are also the permanent deviatoric strains. They also should be taken into account in the compaction model. And finally, the model should work also for a large number of loading cycles.

In this paper, we present an experimental analysis devoted to developments of permanent strains due to cyclic loadings of granular soils. The starting point

are the experimental results obtained from the tests performed in the cyclic triaxial apparatus. Then, a theoretical analysis of experimental data is performed, and semi-empirical constitutive equations proposed.

## 2. Notation and Experimental Program

The experiments described in this paper were performed in the cyclic triaxial apparatus *Enel-Hydro* manufactured in Italy. The system enables sinusoidal cyclic changes of the vertical stress, with the frequency up to 2 Hz, and local measurements of both the vertical and horizontal strains. The strains were measured by the proximity transducers with the accuracy of  $10^{-5}$ . The diameter of a soil sample was 70 mm, and its height was 140 mm.

The model “Skarpa” sand was used in experimental investigations. This is the quartz sand, characterized by the following parameters: median size of grains  $D_{50} = 420 \mu\text{m}$ ; uniformity coefficient  $C_U = 2.5$ ; specific gravity  $G = 2.65$ ; maximum and minimum void ratios  $e_{\max} = 0.677$  and  $e_{\min} = 0.432$  respectively; angles of internal friction of loose and dense sand  $\phi = 34^\circ$  and  $41^\circ$  respectively. The experiments were performed on dry samples.

The following stress and strain variables will be applied in the present paper:

$$p = \frac{1}{3}(\sigma_1 + 2\sigma_3), \quad (1)$$

$$q = \sigma_1 - \sigma_3, \quad (2)$$

$$\varepsilon_v = \varepsilon_1 + 2\varepsilon_3, \quad (3)$$

$$\varepsilon_q = \frac{2}{3}(\varepsilon_1 - \varepsilon_3), \quad (4)$$

where  $\sigma_1$  = vertical stress;  $\sigma_3$  = horizontal stress;  $\varepsilon_1$  = vertical strain;  $\varepsilon_3$  = horizontal strain. The symbols appearing in Eqs. (1)–(4) have the following meaning:  $p$  = mean stress;  $q$  = deviatoric stress;  $\varepsilon_v$  = volumetric strain;  $\varepsilon_q$  = deviatoric strain. We shall also introduce a non-dimensional stress variable:

$$\eta = \frac{q}{p}. \quad (5)$$

The experimental program has included the cyclic loading tests around different initial constant stress states, as shown in Fig. 2. During the cyclic loading experiments, only the vertical stress  $\sigma_1$  was cyclically changed, whilst the horizontal stress  $\sigma_3$  (pressure in the cell) was kept constant:

$$\sigma_1 = \sigma_1^0 + \Delta\sigma_1^c \sin \omega t, \quad (6)$$

$$\sigma_3 = \sigma_3^0 = \text{const}, \quad (7)$$

where  $\sigma_1^0$  and  $\sigma_3^0$  denote the initial constant stress components;  $\Delta\sigma_1^c$  = vertical cyclic stress amplitude;  $\omega = 2\pi f$  = frequency of cyclic loading;  $f = 0.5 \div 1$  Hz.

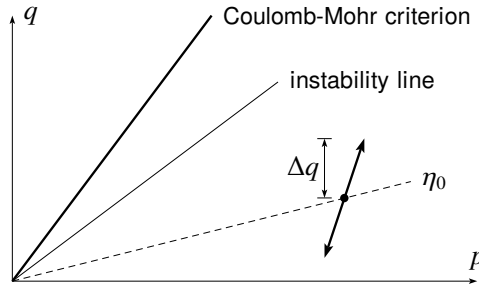


**Fig. 2.** Cyclic stress path in the  $p, q$  space

Fig. 2 shows the cyclic stress path around some initial constant stress state, denoted by  $p_0$  and  $q_0$ , in the stress space  $p, q$ . It follows from Eqs. (1), (2), (6) and (7) that:

$$p = \frac{1}{3}(\sigma_1^0 + 2\sigma_3^0) + \frac{1}{3}\Delta\sigma_1^c \sin \omega t = p_0 + \frac{1}{3}\Delta\sigma_1^c \sin \omega t, \quad (8)$$

$$q = \sigma_1^0 - \sigma_3^0 + \Delta\sigma_1^c \sin \omega t = q_0 + \Delta\sigma_1^c \sin \omega t. \quad (9)$$

The above equations show that both the mean and deviatoric stresses are subjected to cyclic changes, which is reflected by the “geotechnical” cyclic stress path shown in Fig. 2. It was impossible, in the cyclic triaxial apparatus used in experimental work, to apply just pure cyclic shearing, i.e. the vertical cyclic stress path for  $p = \text{const}$ .

The experiments were performed for three different values of the cyclic stress amplitude  $\Delta\sigma_1^c$ , which were roughly equal to 12.5, 25 and 50 kPa. In particular experiments these values were slightly different, due to construction of the triaxial apparatus. The cyclic loading was carried out up to  $N = 10^4$  cycles.

The experiments were performed also around different mean constant stresses, characterized by different values of the non-dimensional stress  $\eta_0$ . The first group of experiments dealt with the case  $\eta_0 = 0$ , which means  $q_0 = 0$ . In the second group of experiments, the cyclic loading was carried out around the instability line, defined by  $\eta_0 = \eta' = 0.96$ . The value of  $\eta'$  was determined experimentally. The third group of experiments dealt with the cyclic loading around  $\eta_0 = \eta'/2$ . All experiments were performed for  $p_0 = 200$  kPa.

### 3. Experimental Results

#### 3.1. The Case of $\eta_0 = 0$

Fig. 3 shows the permanent volumetric strains that develop in a medium dense sand ( $e_0 = 0.53$ ) due to the cyclic loading at different cyclic shear stress amplitudes, namely 13, 26 and 52 kPa. Similar results, obtained from 7 different experiments

performed on samples characterized by similar initial void ratios, are shown in Fig. 4. Fig. 5 shows the permanent deviatoric strains that develop in these samples due to cyclic loading.

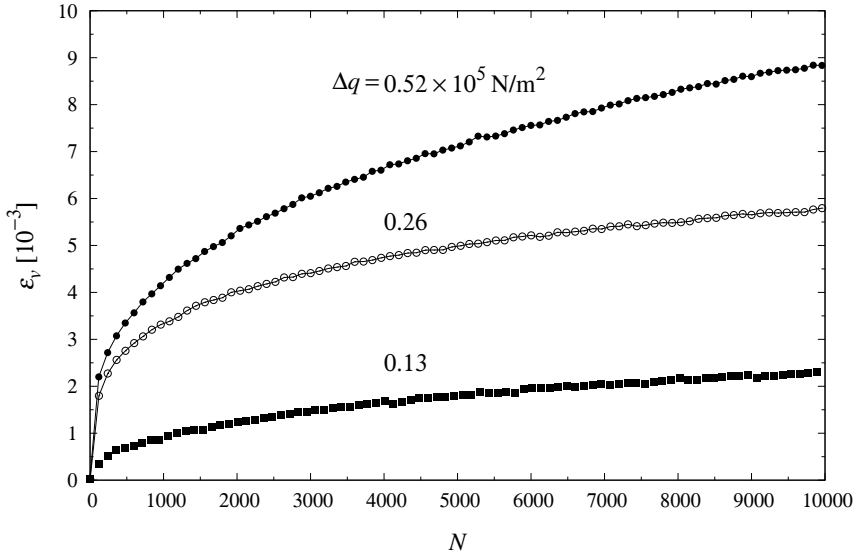


Fig. 3. Compaction curves for  $\eta_0 = 0$

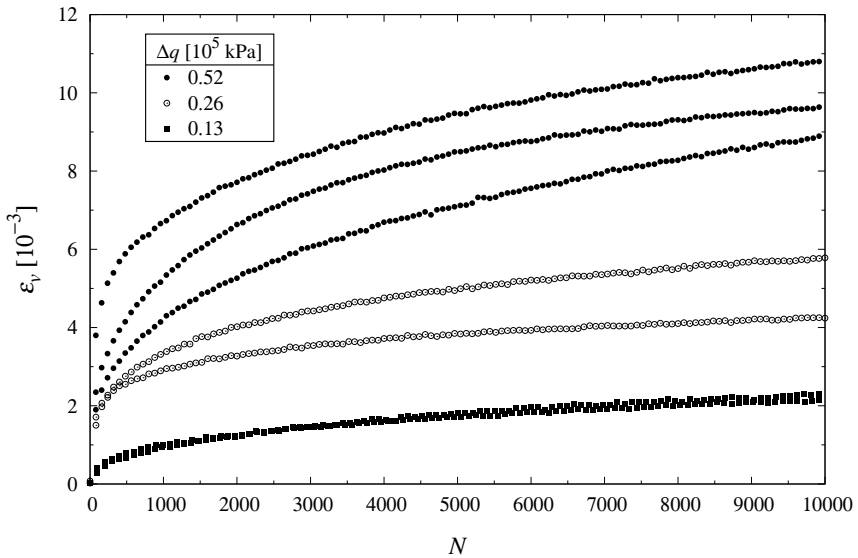


Fig. 4. Compaction curves for  $\eta_0 = 0$  obtained from 7 different experiments, at different cyclic stress amplitudes

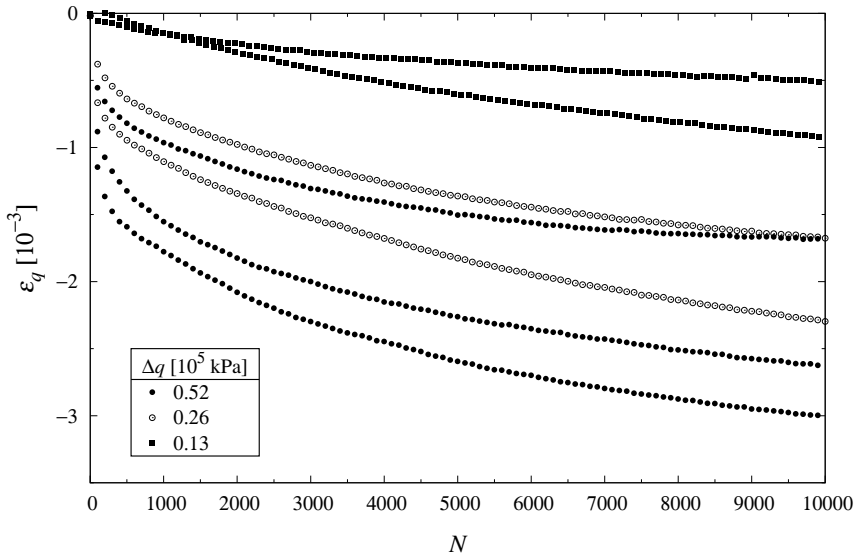


Fig. 5. Permanent deviatoric strains developed in sand due to cyclic loading, cf. Fig. 4

Fig. 6 illustrates the amplitudes of cyclic deviatoric strains  $\Delta\varepsilon_q = \frac{2}{3}\Delta(\varepsilon_1 - \varepsilon_3)$ , for the experiments corresponding to Figs. 4 and 5.

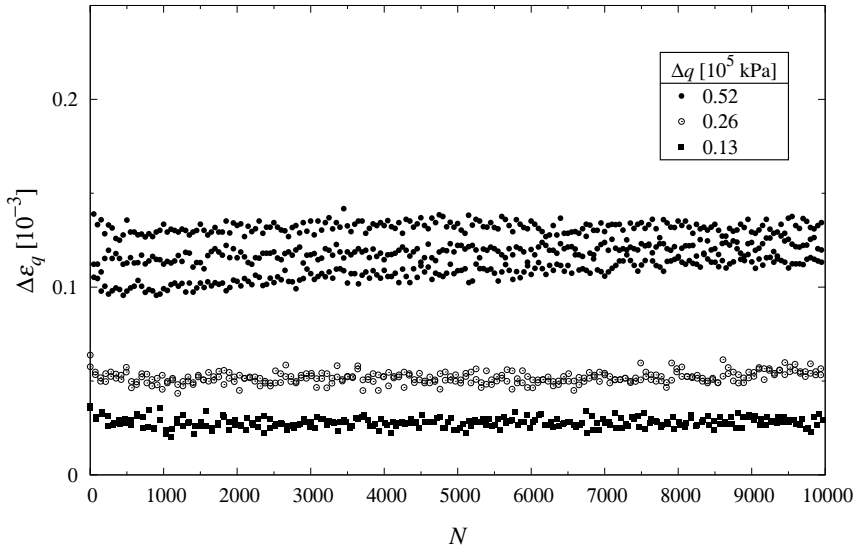
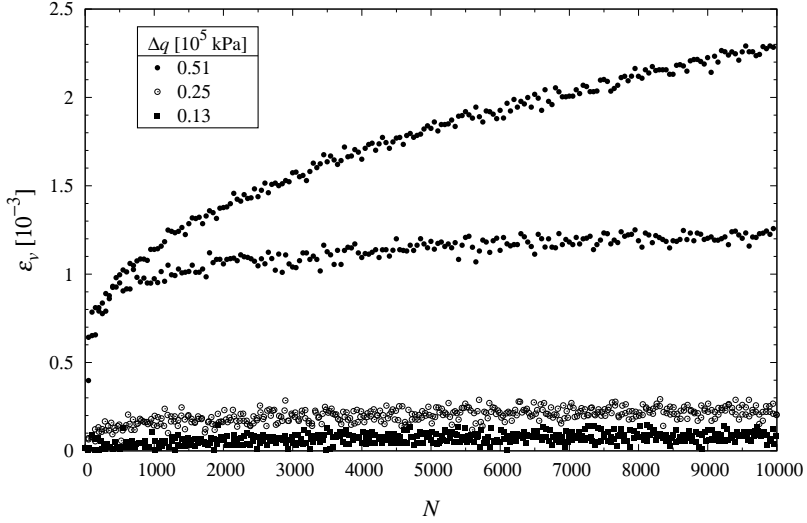


Fig. 6. The amplitudes of cyclic deviatoric strains caused by different cyclic stress amplitudes

### 3.2. The Case of $\eta_0 \neq 0$

Figs. 7 and 8 show the compaction curves obtained from the cyclic shearing at different cyclic stress amplitudes, for two values of  $\eta_0$ , namely  $\eta_0 = \eta'/2$  and  $\eta_0 = \eta'$ .



**Fig. 7.** Compaction for  $\eta_0 = \eta'/2$  obtained from 6 different experiments, at different cyclic stress amplitudes

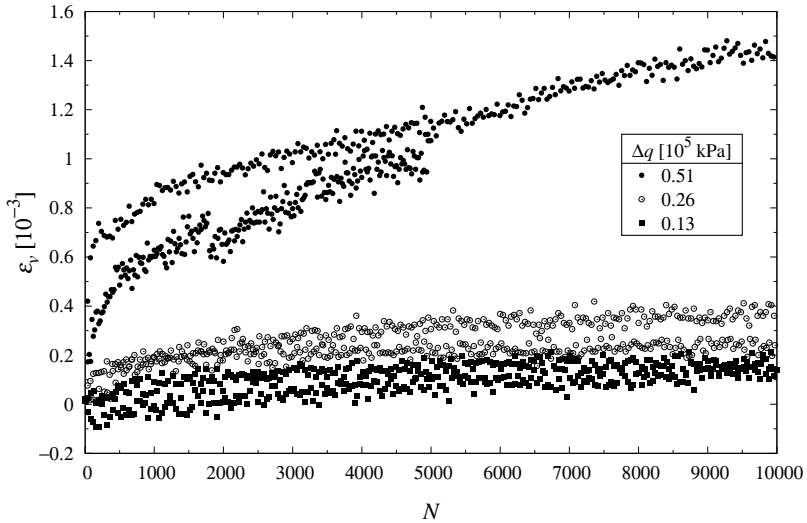


**Fig. 8.** Compaction for  $\eta_0 = \eta'$  obtained from 6 different experiments, at different cyclic stress amplitudes

#### 4. Description of Permanent Volumetric Strains

The aim of analysis presented below is to find a common compaction curve for sand that is cyclically loaded in triaxial conditions, as shown in Fig. 2. A general form of such a curve is the following:

$$\varepsilon_v^p = \varepsilon_v^p(\Delta q, N, \xi), \quad (10)$$

where  $\xi = \eta_0/\eta'$  defines the initial (static) stress state, around which the cyclic stress amplitude oscillates.

##### 4.1. Volumetric Strains After a Large Number of Cycles ( $N = 10^4$ )

Table 1 shows average volumetric strains  $\varepsilon_v^*$  that have been developed after a large number of loading cycles  $N = 10^4$ , for three values of the cyclic stress amplitude  $\Delta q$ , and four values of parameter  $\xi$ . The effect caused by the first two cycles has not been taken into account as during these cycles the soil sample adapts to the cyclic loading conditions. Wichtmann et al (2005) also suggest that these cycles should be considered separately. The data presented in Table 1 correspond to the mean effective stress  $p'_0 = 2 \times 10^5 \text{ N/m}^2$ .

The first conclusion that follows from Table 1 is obvious: increase of  $\Delta q$  results in larger densification. The second conclusion is that increasing values of  $\xi$  correspond to decreasing values of corresponding densification, for the same value of  $\Delta q$ . Note that some results, corresponding to  $\xi = 1$ , deviate from this trend, but it should be remembered that  $\xi = 1$  corresponds to the instability line, so we may expect some irregular reaction of the soil.

**Table 1.** Permanent volumetric strains after  $N = 10^4$  cycles ( $\varepsilon_v^*$  expressed in unit  $10^{-3}$ ,  $\Delta q$  in unit  $10^5 \text{ N/m}^2$ )

$\xi$	$\Delta q$		
	0.52	0.26	0.13
0.0	9.767	5.025	2.25
0.26	3.11	0.76	–
0.5	1.76	0.207	0.073
1.0	1.225	0.325	0.145

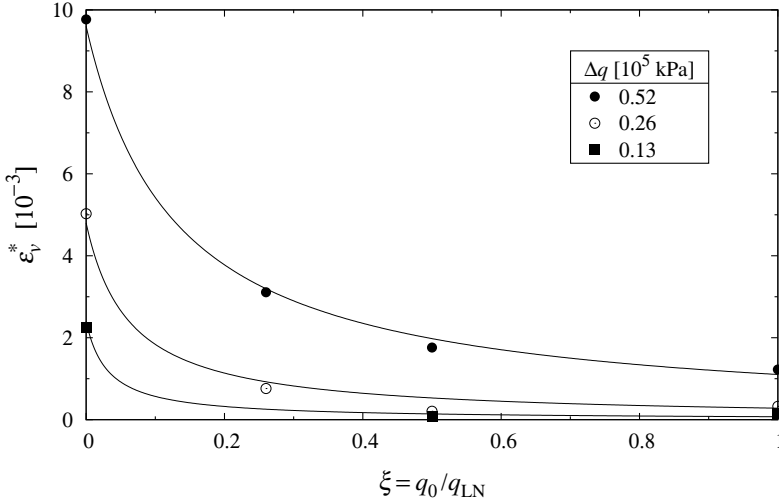
##### 4.2. Analytical Approximation of Experimental Data

Fig. 9 shows an approximation of the results from Table 1, in the  $\xi, \varepsilon_v^*$  plane, for each value of  $\Delta q$ . Respective curves can be approximated by the following simple formula:

$$\varepsilon_v^* = \frac{a}{\xi + b}, \quad (11)$$



where  $a = a(\Delta q)$  and  $b = b(\Delta q)$  are certain functions of the cyclic stress amplitude. Table 2 shows the values of these coefficients for different cyclic stress amplitudes.



**Fig. 9.** Relationship between  $\varepsilon_v^*$  and  $\xi$  for different values of  $\Delta q$

**Table 2.** Values of  $a$  and  $b$  for different  $\Delta q$ , corresponding to Fig. 9

$\Delta q$	$a$	$b$
0.52	1.2458	0.1298
0.26	0.2979	0.06207
0.13	0.07448	0.03103

We have tried to fit the data from Fig. 9 into a single (common) curve, using the method of trial and error. It seems that the following approximation leads to reasonable results:

$$a = A\Delta q^2, \quad b = B\Delta q, \tag{12}$$

where  $A$  and  $B$  are some constants. Table 3 shows the values of these coefficients for different cyclic stress amplitudes.

**Table 3.** Values of the coefficients  $A$  and  $B$  for different cyclic stress amplitudes  $\Delta q$

$\Delta q$	$A$	$B$
0.52	4.607	0.25
0.26	4.41	0.24
0.13	4.41	0.24

The values of  $A$  and  $B$  are almost the same for different values of  $\Delta q$ , which means that they can be treated as a kind of material constants indeed. Their mean values are the following:  $A = 4.48$ ,  $B = 0.243$ .

Eqs. (11) and (12) lead to the following formula:

$$\frac{\varepsilon_v^*}{\Delta q} = \frac{A}{\frac{\xi}{\Delta q} + B}, \quad (13)$$

which can be presented as a single curve in the space  $\xi/\Delta q, \varepsilon_v^*/\Delta q$ , as shown in Fig. 10.

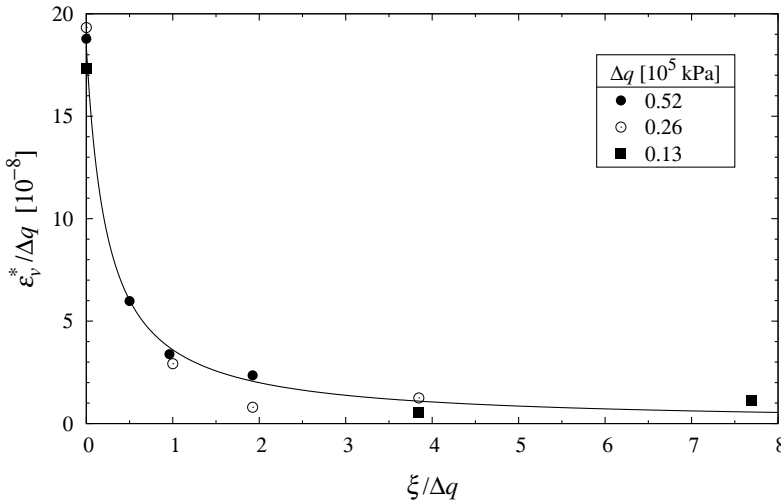


**Fig. 10.** A common compaction curve illustrating dependence of  $\varepsilon_v^*/\Delta q$  on  $\xi/\Delta q$ , see Eq. (13)

### 4.3. Common Compaction Curves

In the previous Section, the empirical relation (13) between  $\varepsilon_v^*$  and  $\xi$  and  $\Delta q$  was derived for the case of large number of loading cycles  $N = 10^4$ . This equation ensures that the empirical results corresponding to different values of  $\xi$  and  $\Delta q$  can be represented in the form of a single curve, as shown in Fig. 10. Now, we shall make use of Eq. (13) in order to construct a common compaction curve in a general form:

$$\varepsilon_v = \varepsilon_v^* f(N), \quad (14)$$

where  $\varepsilon_v^*$  is given in Eq. (13), and  $f(N)$  is a certain function of loading cycles, such that  $f(N = 10^4) = 1$ .

The most simple shape of this function is the following:

$$f(N) = \beta \ln(1 + \alpha N), \quad (15)$$

where  $\alpha$  and  $\beta$  are certain constants. For the data analysed in the present paper, one obtains:  $\alpha = 0.02577$ ;  $\beta = 0.18$ .

Fig. 11 illustrates the common compaction curve, defined by Eqs. (14) and (15).

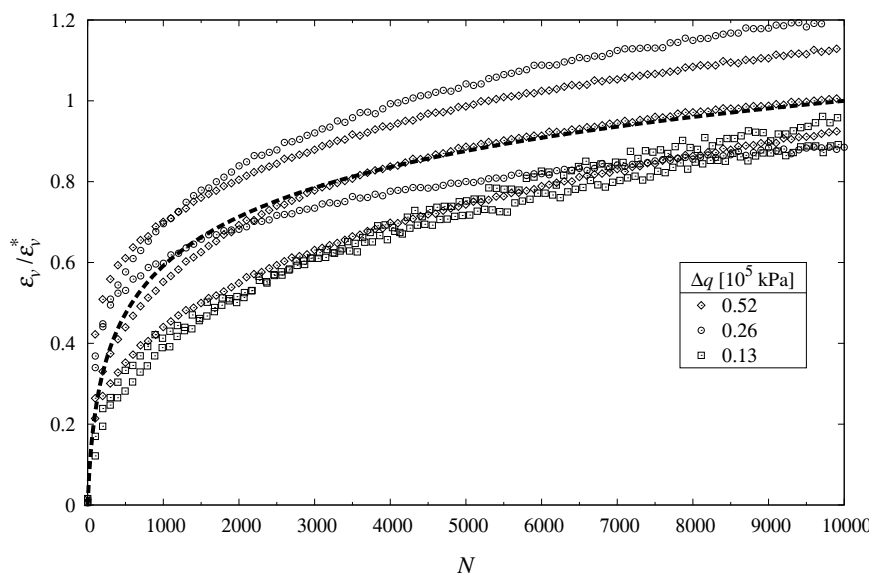


**Fig. 11.** Common compaction curve, see Eqs. (14) and (15)

Eqs. (14) and (15) lead to the following formula:

$$\varepsilon_v = Y \ln(1 + \alpha N), \quad (16)$$

where  $Y = \varepsilon_v^* \beta$ .

Differentiation of Eq. (16) with respect to  $N$  leads to the following incremental equation:

$$d\varepsilon_v = \left[ \frac{dY}{dN} \ln(1 + \alpha N) + \frac{\alpha Y}{1 + \alpha N} \right] dN. \quad (17)$$

## 5. Accumulated Deviatoric Strains

A similar procedure, as that described previously, can be applied in order to describe the accumulated deviatoric strains that develop during the cyclic loading. Usually such strains are ignored, as sands are treated as initially isotropic materials, see the state-of-the-art paper by Sawicki and Mierczyński (2006).

Table 4 presents mean deviatoric strains  $\varepsilon_q = (2/3)(\varepsilon_1 - \varepsilon_3)$  accumulated after a large number of loading cycles  $N = 10^4$ .

**Table 4.** Accumulated deviatoric strains after  $N = 10^4$   
( $\varepsilon_q^*$  expressed in unit  $10^{-3}$ )

$\xi$	$\Delta q$		
	0.52	0.26	0.13
0.0	-2.82	-2.0	-0.72
0.25	0.353	0.043	–
0.5	0.95	0.173	0.09
1.0	2.7	1.17	0.73

Similarly as in the case of volumetric strain, it can be shown that the data from Table. 4 may be presented in the form of a common line:

$$\frac{\varepsilon_q^*}{\Delta q} = \frac{A_q}{\xi + B_q} + C_q, \quad (18)$$

where:  $A_q = -4.9$ ,  $B_q = 0.32$  and  $C_q = 8.5$ . Fig. 12 shows the function (18) and experimental data in  $\xi$  and  $\varepsilon_q^*/\Delta q$  coordinates.

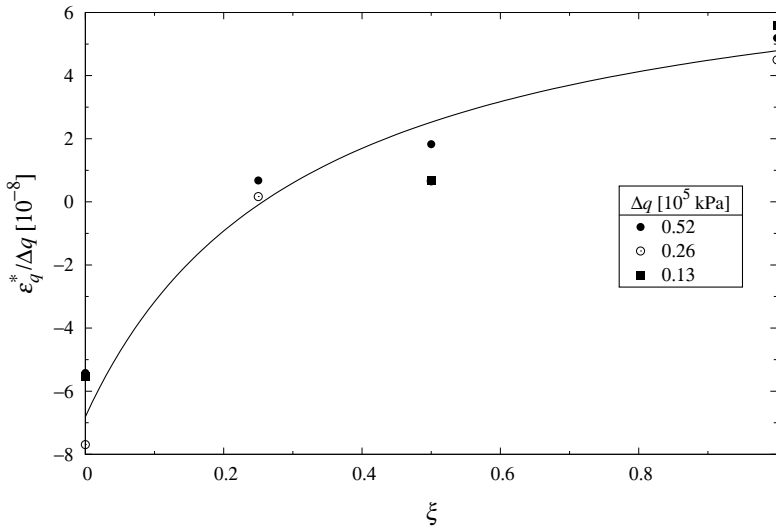


**Fig. 12.** Dependence of  $\varepsilon_q^*/\Delta q$  on  $\xi$  – analytical approximation versus experimental data

## 6. Summary

The key results presented in this paper can be summarized as follows:

- a) In the paper the analytical approximation of experimental data illustrating the deformation of sand subjected to large number of loading cycles is proposed. Accumulated volumetric and deviatoric strains were described by Eqs. (7) and (12), respectively. These strains are the function of three independent variables: amplitude of cyclic stress deviator  $\Delta q$ ; number of loading cycles  $N$  and initial stress state defined by parameter  $\xi$ . Analytical relations were chosen in such a way, in order to obtain possibly the best agreement between analytical approximations and experimental data for  $N = 10^4$ . The shape of the approximations can be controlled by a selection of function  $f(N)$ .
- b) The relations proposed can be transformed to the incremental form, as it was shown in Section 3.3, see Eq. (9), so as it would be possible to apply them for a given cyclic loading history  $\Delta q = \Delta q(N)$ .
- c) There is some scatter in the experimental data, however it is a standard response in the case of granular media, see Sawicki and Chylicki (2009). The analytical approximations of these data correspond obviously to averaged functions. In these approximations, some small cyclic fluctuations of mean stress caused by application of standard “geotechnical” cyclic stress path have been ignored. Such stress path is forced by technical limitations of the triaxial apparatus applied.
- d) Accumulation curves of strains proposed in this paper refer to the large number of loading cycles. Analytical approximations differ in the form from previously proposed “common compaction curves”, however they have a “common” form too, i.e. a common curve for experimental results corresponding to various values of independent variables ( $\Delta q$ ,  $N$  and  $\xi$ ). Original “common compaction curve” is still valid, however for a rather low number of loading cycles, say  $N < 100$ , as it was shown by earlier investigations, see Świdziński and Mierczyński (2006).
- e) In the proposed analytical relations (7) and (12), one of the independent variables is  $\Delta q$ , whereas in classical compaction theory this variable was replaced by another one representing the cyclic strain amplitude.
- f) The dependence of accumulated deformations on the initial stress state defined by parameter  $\xi$  was also included in the approach proposed. Such dependence was not considered by other authors. It should also be noted that the accumulated deviatoric strains change the sign after exceeding some ultimate value of  $\xi$ , which approximately is equal to 0.25.

## Acknowledgement

Research presented in this paper was supported by the Polish Ministry of Science and Higher Education: research grant No. 4 T07A 028 30.

## References

- Ishihara K. (1996) *Soil Behaviour in Earthquake Geotechnics*, Clarendon Press, Oxford.
- Martin G. R., Finn W. D. L. and Seed H. B. (1975) Fundamentals of liquefaction under cyclic loading, *J. Geot. Eng. Div., ASCE*, **101**, GT5, 423–428.
- Nemat-Nasser S. and Shokoh A. (1979) A unified approach to densification of cohesionless sand in cyclic shearing, *Canadian Geot. J.*, **16**, 659–678.
- Niemunis A. (2003) *Extended Hypoplastic Models For Soils*, Gdańsk University of Technology.
- Sawicki A. (1987) An engineering model for compaction of sand under cyclic loading, *Engineering Transactions*, **35** (4), 677–693.
- Sawicki A., Mierczyński J. (2006) Development in modelling liquefaction of granular soils, caused by cyclic loads, *Applied Mechanics Reviews*, **59**, 91–106.
- Sawicki A., Świdziński W. (2007) Simple mathematical model for assessment of seismic-induced liquefaction of soils. *Journal of Waterway, Port, Coastal and Ocean Engineering, ASCE*, **133** (1), 50–54.
- Sawicki A., Chybicki W. (2009) On accuracy of prediction of pre-failure deformations of granular soils, *Computers and Geotechnics*, in press (on line, doi:10.1016/j.compgeo.2009.03.008).
- Świdziński W., Mierczyński J. (2006) Compaction of sands in cyclic triaxial conditions (in Polish), *Zeszyty Naukowe Politechniki Białostockiej*, **28**, 299–314.
- Wichtmann T., Niemunis A. and Triantafyllidis Th. (2005) Strain accumulation in sand due to cyclic loading: drained triaxial tests, *Soil Dynamics and Earthquake Engng.*, **25**, 967–979.